

EXPLOITING MUTUAL COUPLING BY MEANS OF ANALOG-DIGITAL ZERO FORCING

Ang Li and Christos Masouros

Dept. of Electronic and Electrical Eng., University College London, London, UK

Email: {ang.li.14, c.masouros}@ucl.ac.uk

ABSTRACT

In this paper, the mutual coupling effect among antenna elements for the downlink multiuser multiple-input-single-output (MU-MISO) is studied. Different from conventional knowledge that the mutual coupling effect usually degrades the system performance, a joint analog-digital precoding scheme is proposed so that the system can benefit from this effect. Linear precoding approaches are applied in the digital domain, while in the analog domain, convex optimization is applied to determine the value of each load impedance such that the resulting noise amplification factor for the precoder is minimized. Simulation results show that the proposed analog-digital precoding schemes can achieve a significant performance gain over conventional precoding approaches with fixed mutual coupling.

Index Terms— MIMO, precoding, mutual coupling, analog-digital processing, optimization.

1. INTRODUCTION

During the past few years, multiple-input-multiple-output (MIMO) techniques have proved to achieve significant performance gains over traditional single-input-single-output (SISO) systems, and precoding techniques that can transfer the computational complexity from the user side to the base station side have been extensively studied [1]. The capacity achieving dirty paper coding (DPC) has been proposed in [2] to pre-subtract the interference before transmission. However, DPC is difficult to implement due to its impractical assumption and high computational complexity. Therefore, suboptimal non-linear techniques such as Tomlinson-Harshima precoding (THP) and vector perturbation (VP) have been proposed [3]-[5]. On the other hand, linear precoding approaches are receiving an increasing research attention due to their low complexity. Zero-forcing (ZF) precoding scheme can provide the least complexity [6], while the performance is far from optimum. Regularized ZF (RZF) proposed in [7] can improve the performance of ZF by introducing a regularization factor. A correlation rotation linear scheme is proposed in [8] which exploits the constructive interference to further benefit the system performance. Compared to linear schemes, while non-linear approaches can provide rate benefits, they can be highly computationally expensive. This is especially true when the number of antennas increases [9]-[11]. Therefore, due to the complexity benefits of linear approaches, we will focus on linear precoding schemes in this paper.

Most existing studies on precoding schemes usually assume an ideal antenna array, which means no spatial correlation or mutual coupling is considered among antenna elements. Nevertheless, in practice when the antenna spacing between antenna element is small,

the spatial correlation and mutual coupling effect cannot be ignored [9][12]. Experimental studies have been conducted to investigate the spatial correlation [13]-[16], and the designs of precoding schemes in spatially correlated channels can be found in [17][18]. The effect of mutual coupling on the system performance is investigated in [19]-[21]. These studies have shown that the existence of mutual coupling effect usually degrades the detection performance. In order to alleviate this performance loss, mutual coupling compensation techniques have been proposed [22]-[28]. In [22], by adding parasitic elements to the antenna array, a reverse coupling effect can be formulated and alleviate the effect of mutual coupling. [23] proposes a novel structure to suppress the mutual coupling effect by adding a U-shaped microstrip, and has tested its effectiveness. In [24], the mutual coupling effect at low-terahertz (THz) frequencies is studied, and a mantle cloaking method is applied to reduce the mutual coupling between strip dipole antennas. In [25], the mutual coupling compensation is studied for both transmitting antenna arrays and receiving antenna arrays, where the calculation of the mutual coupling compensation matrices is given. We note that most of the above compensation schemes are not from a signal processing perspective.

In this paper, we propose a joint analog-digital precoding scheme that exploits the mutual coupling effect among antenna elements rather than compensates for this effect, to further improve the system performance. In the proposed scheme, it is assumed that each antenna is equipped with a tunable load impedance (for example a varactor) such that the mutual coupling effect can be controlled by tuning the value of each load impedance. In the digital domain, conventional linear precoding is applied, while in the analog domain, convex optimization is applied to facilitate the analog precoding. By judiciously picking the value of each load impedance, the noise amplification factor for the proposed precoder can be minimized, and an improved detection performance can be expected. Realistic constraints are considered for the optimization problems, and we also discuss the practical implementation of the proposed schemes. In the numerical results, it will be shown that with the proposed precoding schemes, the mutual coupling effect can actually benefit the system and an improved detection performance can be observed.

Notations: a , \mathbf{a} , and \mathbf{A} denote scalar, vector and matrix respectively. $\mathbb{E}\{\cdot\}$, $(\cdot)^T$, $(\cdot)^H$, $(\cdot)^{-1}$ and $tr(\cdot)$ denote expectation, transpose, conjugate transpose, inverse and trace of a matrix respectively. $\|\cdot\|$ denotes the Frobenius norm and \mathbf{I} is the identity matrix. $\mathcal{C}^{n \times n}$ represents $n \times n$ matrix in the complex set and $diag(\cdot)$ denotes the conversion of a vector into a diagonal matrix with the vector values on its main diagonal. $\Re(\cdot)$ and $\Im(\cdot)$ denote the real part and imaginary part of a complex number, respectively.

2. DOWNLINK SYSTEM AND CHANNEL MODEL

A MU-MISO downlink system is considered where a base station (BS) with N_t antennas communicates with K users simultaneously

This work was supported by the Royal Academy of Engineering, UK, the Engineering and Physical Sciences Research Council (EPSRC) project EP/M014150/1, and the China Scholarship Council (CSC).

and it is assumed that $K \leq N_t$. Before transmission in the wireless environment, the BS processes the transmit symbol vector with a precoding matrix, and the signal vector at the receiver side can be expressed as

$$\mathbf{y} = \mathbf{H}\mathbf{Z}\mathbf{x} + \mathbf{n} = \frac{1}{f}\mathbf{H}\mathbf{Z}\mathbf{P}\mathbf{s} + \mathbf{n}, \quad (1)$$

where $\mathbf{s} \in \mathcal{C}^{K \times 1}$ is the data symbol vector with the assumption that $\mathbb{E}\{\mathbf{s}\mathbf{s}^H\} = \mathbf{I}$ and $\mathbf{P} \in \mathcal{C}^{N_t \times K}$ is the precoding matrix. $\mathbf{x} = \frac{1}{f} \cdot \mathbf{P}\mathbf{s}$ is the precoded signal to transmit and f is the noise amplification factor that ensures the average transmit power is not changed after precoding. $\mathbf{H} \in \mathcal{C}^{K \times N_t}$ is the channel matrix and we assume perfect channel knowledge for the BS. Each element of $\mathbf{n} \in \mathcal{C}^{K \times 1}$ is assumed to be the additive white Gaussian noise (AWGN) with zero mean and variance σ^2 . \mathbf{Z} is the mutual coupling matrix at the transmitter side that will be introduced in the following.

When the antenna spacing is small, the effect of transmit spatial correlation should also be considered in the channel model. Therefore, a semi-correlated geometric non-line of sight (NLOS) Rayleigh flat fading channel model is assumed in this paper [9][12], where the correlation is considered at the transmitter side. We then model the channel as

$$\mathbf{H} = [\mathbf{h}_1^T, \mathbf{h}_2^T, \dots, \mathbf{h}_K^T]^T, \quad (2)$$

where $\mathbf{h}_k \in \mathcal{C}^{1 \times N_t}$ is the channel vector for user k and can be expressed as [9][12]

$$\mathbf{h}_k = \mathbf{g}_k \mathbf{A}_k, \quad (3)$$

where each element in \mathbf{g}_k follows the standard complex Gaussian distribution $\mathcal{CN}(0, 1)$ that forms the Rayleigh component. $\mathbf{A}_k \in \mathcal{C}^{M \times N_t}$ is the transmit-side steering matrix that contains M steering vectors of the transmit antenna array, where M is the number of directions of departure (DoDs). We assume uniform linear arrays (ULAs) in this paper, whereas \mathbf{A}_k can be modeled as

$$\mathbf{A}_k = \frac{1}{\sqrt{M}} [\mathbf{a}^T(\phi_{k,1}), \mathbf{a}^T(\phi_{k,2}), \dots, \mathbf{a}^T(\phi_{k,M})]^T. \quad (4)$$

In (4), $\mathbf{a}(\phi_{k,i}) \in \mathcal{C}^{1 \times N_t}$ is given by

$$\mathbf{a}(\phi_{k,i}) = [1, e^{j2\pi d \sin \phi_{k,i}}, \dots, e^{j2\pi(N_t-1)d \sin \phi_{k,i}}], \quad (5)$$

where d is the antenna spacing normalized by the carrier wavelength, and $\phi_{k,i}$ denotes the angles of departure (AoDs) which is assumed to be randomly and independently distributed in $[-\Phi, \Phi]$ with a uniform distribution.

In (1), $\mathbf{Z} \in \mathcal{C}^{N_t \times N_t}$ is the mutual coupling matrix, and we can derive the mutual coupling matrix with tunable loads based on [9][29] as

$$\mathbf{Z}(\mathbf{z}_L) = [z_A \cdot \mathbf{I} + \text{diag}(\mathbf{z}_L)] [\mathbf{\Gamma} + \text{diag}(\mathbf{z}_L)]^{-1}, \quad (6)$$

where z_A is the antenna impedance and $\mathbf{z}_L = [z_{L_1}, z_{L_2}, \dots, z_{L_{N_t}}]^T$ is the load impedance vector to be optimized. $\mathbf{\Gamma}$ is the mutual impedance matrix and can be expressed as

$$\mathbf{\Gamma} = \begin{bmatrix} z_A & z_{m_1} & z_{m_2} & \cdots & z_{m_{N_t-1}} \\ z_{m_1} & z_A & z_{m_1} & \ddots & \vdots \\ z_{m_2} & z_{m_1} & \ddots & \ddots & z_{m_2} \\ \vdots & \ddots & \ddots & \ddots & z_{m_1} \\ z_{m_{N_t-1}} & \cdots & z_{m_2} & z_{m_1} & z_A \end{bmatrix}, \quad (7)$$

where z_{m_k} denotes the mutual impedance of two antenna elements with the distance of $k \cdot d$. The value of z_A and z_{m_k} can be obtained by the induced electromagnetic-field (EMF) method based on the antenna spacing d , shown in Chapter 8 of [20].

3. PROPOSED ANALOG-DIGITAL PRECODING

In this section, the proposed scheme is introduced based on the ZF precoder where each antenna element is equipped with a varactor as load impedance so that the mutual coupling can be controlled. The idea is to manipulate the value of each load impedance by optimization to minimize the noise amplification factor f of the precoder. To exploit the mutual coupling effect, based on (1) we construct the precoding matrix \mathbf{P} as

$$\mathbf{P} = \mathbf{Z}^{-1} \mathbf{H}^H (\mathbf{H} \mathbf{H}^H)^{-1}, \quad (8)$$

which is based on the concept of ZF and can fully eliminate the multi-user interference. Then, the precoded signal vector \mathbf{x} can be obtained as

$$\mathbf{x} = \frac{1}{f} \cdot \mathbf{P}\mathbf{s} = \frac{1}{f} \cdot \mathbf{Z}^{-1} \mathbf{W}\mathbf{s}, \quad (9)$$

where we denote $\mathbf{W} = \mathbf{H}^H (\mathbf{H} \mathbf{H}^H)^{-1}$ for simplicity and the noise amplification factor f is given by

$$f = \|\mathbf{P}\| = \sqrt{\text{tr}(\mathbf{P}\mathbf{P}^H)}. \quad (10)$$

At the receiver, by incorporating (9) into (1), the received signal vector can be obtained as

$$\mathbf{y} = \frac{1}{f} \cdot \mathbf{H}\mathbf{Z}\mathbf{Z}^{-1} \mathbf{W}\mathbf{s} + \mathbf{n} = \frac{1}{f} \cdot \mathbf{s} + \mathbf{n}. \quad (11)$$

Before demodulation, the received signal vector needs to be scaled back to eliminate the factor f , and the rescaled signal vector can then be obtained as

$$\mathbf{r} = f \cdot \mathbf{y} = \mathbf{s} + f \cdot \mathbf{n}. \quad (12)$$

As can be observed, with the proposed precoder, the mutual coupling effect is fully eliminated, while it still has an impact on the precoding matrix and the noise amplification factor f . Therefore, by optimizing each value of the load impedance, the noise amplification factor f can be minimized, and a better system performance can be achieved. Therefore, we pursue the following optimization problem

$$\mathcal{P}_0 : \min_{\mathbf{z}_L} \|\mathbf{Z}^{-1} \mathbf{W}\|^2. \quad (13)$$

To solve this optimization problem, we first study the inverse of the mutual coupling matrix. Based on (6), \mathbf{Z}^{-1} can be obtained as

$$\mathbf{Z}^{-1} = \{ [z_A \cdot \mathbf{I} + \text{diag}(\mathbf{z}_L)] [\mathbf{\Gamma} + \text{diag}(\mathbf{z}_L)]^{-1} \}^{-1} = [\mathbf{\Gamma} + \text{diag}(\mathbf{z}_L)] \cdot \text{diag}(\mathbf{z}_T), \quad (14)$$

where we denote $\mathbf{z}_T = [\frac{1}{z_1}, \frac{1}{z_2}, \dots, \frac{1}{z_{N_t}}]^T$ and

$$z_i = z_A + z_{L_i}. \quad (15)$$

By expanding (14), \mathbf{Z}^{-1} is expressed as

$$\mathbf{Z}^{-1} = \begin{bmatrix} 1 & \frac{z_{m_1}}{z_2} & \frac{z_{m_2}}{z_3} & \cdots & \frac{z_{m_{N_t-1}}}{z_{N_t}} \\ \frac{z_{m_1}}{z_1} & 1 & \frac{z_{m_1}}{z_3} & \ddots & \vdots \\ \frac{z_{m_2}}{z_1} & \frac{z_{m_1}}{z_2} & \ddots & \ddots & \frac{z_{m_2}}{z_{N_t}} \\ \vdots & \ddots & \ddots & \ddots & \frac{z_{m_1}}{z_{N_t}} \\ \frac{z_{m_{N_t-1}}}{z_1} & \cdots & \frac{z_{m_2}}{z_{N_t-2}} & \frac{z_{m_1}}{z_{N_t-1}} & 1 \end{bmatrix}. \quad (16)$$

Then, by denoting

$$\Theta = \text{diag} \left(\frac{z_{m_1}}{z_1}, \frac{z_{m_1}}{z_2}, \dots, \frac{z_{m_1}}{z_{N_t}} \right) = \text{diag} (\theta_1, \theta_2, \dots, \theta_{N_t}), \quad (17)$$

\mathbf{Z}^{-1} can be further decomposed as

$$\mathbf{Z}^{-1} = \mathbf{B}\Theta + \mathbf{I}, \quad (18)$$

where \mathbf{B} is given by

$$\mathbf{B} = \begin{bmatrix} 0 & 1 & \frac{z_{m_2}}{z_{m_1}} & \cdots & \frac{z_{m_{N_t-1}}}{z_{m_1}} \\ 1 & 0 & 1 & \ddots & \vdots \\ \frac{z_{m_2}}{z_{m_1}} & 1 & \ddots & \ddots & \frac{z_{m_2}}{z_{m_1}} \\ \vdots & \ddots & \ddots & \ddots & 1 \\ \frac{z_{m_{N_t-1}}}{z_{m_1}} & \cdots & \frac{z_{m_2}}{z_{m_1}} & 1 & 0 \end{bmatrix}. \quad (19)$$

Finally, by substituting (18) into (13), the optimization problem is transformed into

$$\mathcal{P}_1 : \min_{\Theta} \|\mathbf{B}\Theta\mathbf{W} + \mathbf{W}\|^2, \quad (20)$$

which is a least-square problem and can be efficiently solved by convex optimization tools such as CVX and SeDuMi.

In practical implementation when we employ varactors as load impedances, the real part of the varactors should be positive [30][31], which adds to the constraint of the optimization problem in (20). Based on (15) and (17), each load impedance z_{L_i} can be expressed as a function of the variable θ_i , which is given by

$$z_{L_i} = \frac{z_{m_1}}{\theta_i} - z_A, \quad (21)$$

and the real part of each z_{L_i} should be positive, which can be expressed as

$$\Re(z_{L_i}) \geq 0, \quad \forall i \in \{1, 2, \dots, N_t\}. \quad (22)$$

By substituting (21) into (22), the constraint can be further transformed into

$$\begin{aligned} \Re \left(\frac{z_{m_1}}{\theta_i} \right) &\geq \Re(z_A) \\ \Rightarrow \frac{\Re(\theta_i) \Re(z_{m_1}) + \Im(\theta_i) \Im(z_{m_1})}{\|\theta_i\|^2} &\geq \Re(z_A) \\ \Rightarrow \Re(\theta_i) \Re(z_{m_1}) + \Im(\theta_i) \Im(z_{m_1}) &\geq \|\theta_i\|^2 \Re(z_A). \end{aligned} \quad (23)$$

Combining (20) and (23), the optimization problem with practical constraints can be finally formulated as

$$\begin{aligned} \mathcal{P}_2 : \min_{\Theta} \|\mathbf{B}\Theta\mathbf{W} + \mathbf{W}\|^2 \\ \text{s.t.} \\ \Re(\theta_i) \Re(z_{m_1}) + \Im(\theta_i) \Im(z_{m_1}) &\geq \|\theta_i\|^2 \Re(z_A), \quad \forall i \in \mathcal{I}. \end{aligned} \quad (24)$$

where we denote $\mathcal{I} = \{1, 2, \dots, N_t\}$ for simplicity. With the convex constraint (23), \mathcal{P}_2 can be efficiently solved. Then, the resulting mutual coupling matrix is obtained based on (18) as

$$\mathbf{Z}^* = (\mathbf{B}\Theta^* + \mathbf{I})^{-1}, \quad (25)$$

and the precoding matrix can be expressed as

$$\mathbf{P}^* = (\mathbf{B}\Theta^* + \mathbf{I})\mathbf{W}. \quad (26)$$

Remark: Throughout the derivation ZF precoding scheme is employed, while the proposed scheme directly applies to other precoding schemes by substituting \mathbf{W} with other precoding matrix, and the performance gains can still be gleaned.

4. PRACTICAL IMPLEMENTATION

Based on the derivation of the proposed techniques, it can be observed that inline with conventional precoding techniques, the proposed scheme requires the knowledge of \mathbf{H} to perform the optimization. However, we note that in the presence of mutual coupling, based on channel estimation schemes we can only obtain $\hat{\mathbf{H}} = \mathbf{H}\mathbf{Z}$ at the BS. To extract \mathbf{H} from $\hat{\mathbf{H}}$, we note that the mutual impedance Γ is only dependent on the array structure and does not change, and therefore Γ is typically known to the BS either by EMF method or other experimental measurements such as boundary-value approach and transmission-line method [20]. Before data transmission, we can firstly set each load impedance to a specific value, such as $z_{L_i} = 50\Omega, \forall i \in \{1, 2, \dots, N_t\}$, where we denote the resulting load impedance vector as \mathbf{z}_L^0 and mutual coupling matrix as \mathbf{Z}_0 . Then, we estimate the channel $\hat{\mathbf{H}}$ with the reference \mathbf{Z}_0 at the BS. With Γ and \mathbf{Z}_0 known to the BS, \mathbf{H} can be extracted from $\hat{\mathbf{H}}$, and the proposed scheme can be applied.

Still, the proposed schemes require the adaptation of each load impedance z_{L_i} dependent on the variation of the channels. Therefore, adaptive impedance tuning approaches are necessary. In [32] advanced semiconductor technologies have been introduced and studied, where it is shown that employing semiconductor-based and ferroelectric-based varactors can support a tuning speed as fast as 1-100 ns. An adaptive matching network can then be employed based on an automated impedance tuning unit with ferroelectric varactors to facilitate the proposed schemes. Moreover, the adaptive load impedance for each antenna array has been employed in the recent applications of electronically steerable parasitic array radiators (ESPARs), where the radiation patterns of ESPARs are formed by changing the value of each load impedance on a symbol-by-symbol basis. The successful proof-of-concept experiments for ESPARs have supported the design of the proposed scheme.

Therefore, based on the above the proposed schemes can be applied in practice and are mostly suitable for slow or quasi-static fading channels, where the channels change slowly.

5. SIMULATION RESULTS

To evaluate the performance of the proposed precoding scheme, numerical results based on Monte Carlo simulations have been conducted and presented in this section. The channel model follows (2)-(5) and without loss of generality we assume the number of DoDs $M=50$ and the angle spread $\Phi = \pi/8$. The antenna spacing between antenna elements is assumed to be $d = 0.25$, and we denote $\rho = \frac{1}{\sigma^2}$ as the transmit SNR. Apart from ZF based approaches, RZF based schemes where \mathbf{W} in (9) is substituted with $\mathbf{W}_{RZF} =$

$\mathbf{H}^H \left(\mathbf{H}\mathbf{H}^H + \frac{K}{\rho} \cdot \mathbf{I} \right)^{-1}$ are also simulated. For reasons of clarity the following abbreviations are applied: “ZF (RZF) with MC” for conventional ZF (RZF) precoding scheme with fixed mutual coupling, and “ZF (RZF) A-D” for the proposed analog-digital precoding scheme \mathcal{P}_2 .

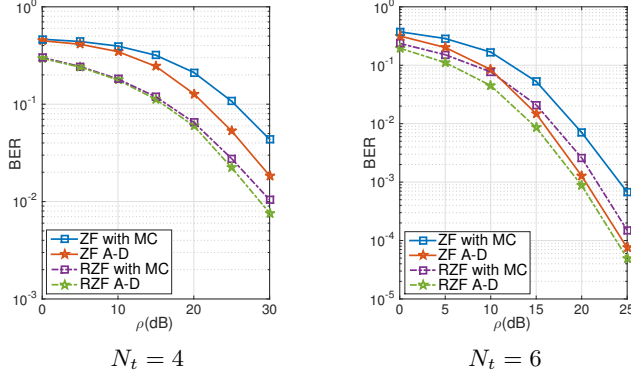


Fig. 1. Bit error rate (BER) v.s. transmit SNR, $K = 4$, QPSK

Fig. 1 compares the bit error rate (BER) performance of the proposed scheme with conventional ZF precoder with respect to the increasing SNR for 1) $K = 4$, $N_t = 4$ and 2) $K = 4$, $N_t = 6$, where QPSK is employed. As can be seen, conventional ZF precoding achieves the worst detection performance because the scheme does not benefit from the mutual coupling effect. The proposed “ZF A-D” achieves an improved performance compared to “ZF with MC” with an SNR gain of 4dB. For both schemes, the performance gain over fixed mutual coupling becomes larger with the increase in the number of transmit antennas.

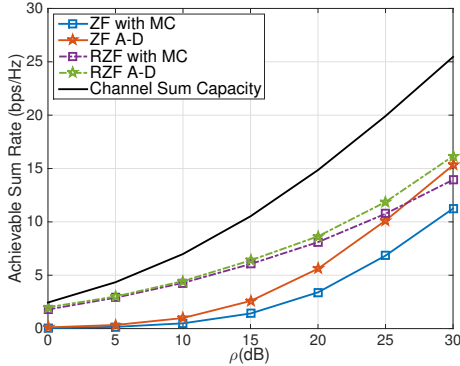


Fig. 2. Achievable sum rate v.s. transmit SNR, $K = N_t = 4$

In Fig. 2, the sum rate for the proposed schemes with respect to the increasing SNR when $K = N_t = 4$ is compared with the unbounded channel sum capacity, which is given by [2][3]

$$C = \mathbb{E} \left\{ \sup_{\mathbf{G} \in \mathbf{A}} \log_2 \left[\det \left(\mathbf{I} + \frac{1}{\sigma^2} \mathbf{H}^H \mathbf{G} \mathbf{H} \right) \right] \right\} \quad (27)$$

where “sup” denotes the supremum function and \mathbf{A} is the set of diagonal $K \times K$ matrices with nonnegative elements that ensures $\text{tr}(\mathbf{G}) = 1$. When equal power transmission is allocated, $\mathbf{G} = (1/K) \cdot \mathbf{I}$. The achievable sum rate for each precoding scheme can be expressed as $R = \sum_{k=1}^K \log_2 (1 + \gamma_k)$, where γ_k is the received

signal-to-noise-ratio (SNR) and can be obtained as

$$\gamma_k^{ZF} = \frac{1}{f^2 \sigma^2},$$

$$\gamma_k^{RZF} = \frac{\left(\sum_{l=1}^K \frac{\lambda_l}{\lambda_l + K \sigma^2} \right)^2}{f_{RZF}^2 K^2 \sigma^2 + K \sum_{l=1}^K \left(\frac{\lambda_l}{\lambda_l + K \sigma^2} \right)^2 - \left(\sum_{l=1}^K \frac{\lambda_l}{\lambda_l + K \sigma^2} \right)^2}, \quad (28)$$

where λ_l is the l -th eigenvalue obtained from the decomposition $\mathbf{H}\mathbf{H}^H = \mathbf{Q}\mathbf{\Lambda}\mathbf{Q}^H$. As can be seen from (28), the proposed schemes optimize the value of each load impedance to minimize the noise amplification factor f , and then the resulting received SNR is maximized, which leads to a better performance compared to conventional ZF with fixed mutual coupling, which is validated by the results in Fig. 2.

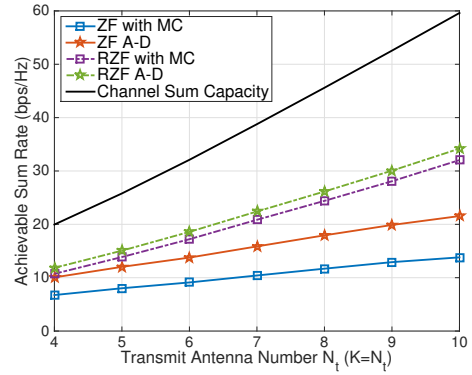


Fig. 3. Achievable sum rate v.s. number of transmit antennas, $K = N_t$, SNR=25dB

Fig. 3 presents the achievable sum rate with respect to the increase in the number of transmit antennas and it is assumed that $K = N_t$. As can be observed, significant performance gains can be observed by the proposed schemes for ZF based schemes, and for RZF based scheme there is also a capacity improvement. The above simulation results have validated that the proposed schemes that exploit the mutual coupling effect can achieve an improved performance compared to conventional precoding schemes. The performance gains are expected to be larger with $N_t > K$.

6. CONCLUSIONS

In this paper, a joint analog-digital precoding scheme that exploits the mutual coupling effect to improve the system performance is proposed. It is shown that by equipping each antenna element with a tunable load impedance, the mutual coupling effect can be controlled and benefit the system performance. By judiciously selecting the value of each load impedance, the noise amplification factor of the precoder can be minimized by convex optimization. The proposed scheme is shown to achieve a significant performance gain over the existing ZF and RZF precoding schemes with fixed mutual coupling, validated by the simulation results. A robust precoder for the imperfect CSI will be the future research focus.

7. REFERENCES

- [1] C. Windpassinger, R. Fischer, T. Vencel, and J. Huber, “Precoding in Multiantenna and Multiuser Communications,”

- IEEE Trans. Wireless Commun.*, vol. 3, no. 4, pp. 1305–1316, July 2004.
- [2] M. Costa, “Writing on Dirty Paper,” *IEEE Trans. Inf. Theory*, vol. IT-29, no. 3, pp. 439–441, May 1983.
 - [3] A. Garcia-Rodriguez and C. Masouros, “Power-Efficient Tomlinson-Harashima Precoding for the Downlink of Multi-User MISO Systems,” *IEEE Trans. Commun.*, vol. 62, no. 6, pp. 1884–1896, April 2014.
 - [4] B. M. Hochwald, C. B. Peel, and A. L. Swindlehurst, “A Vector-Perturbation Technique for Near-Capacity Multiantenna Multiuser Communication-Part ii: Perturbation,” *IEEE Trans. Commun.*, vol. 53, no. 3, pp. 537–544, Mar. 2005.
 - [5] J. Maurer, J. Jalden, D. Seethaler, and G. Matz, “Vector Perturbation Precoding Revisited,” *IEEE Trans. Sig. Process.*, vol. 59, no. 1, pp. 315–328, Jan. 2011.
 - [6] T. Haustein, C. von Helmolt, E. Jorswieck, V. Jungnickel, and V. Pohl, “Performance of MIMO Systems with Channel Inversion,” *Proc. 55th IEEE Veh. Technol. Conf. (VTC)*, vol. 1, pp. 35–39, May 2002.
 - [7] C. B. Peel, B. M. Hochwald, and A. L. Swindlehurst, “A Vector-Perturbation Technique for Near-Capacity Multi-antenna Multiuser Communication-Part i: Channel Inversion and Regularization,” *IEEE Trans. Commun.*, vol. 53, no. 1, pp. 195–202, Jan. 2005.
 - [8] C. Masouros, “Correlation Rotation Linear Precoding for MIMO Broadcast Communications,” *IEEE Trans. Sig. Process.*, vol. 59, no. 1, pp. 252–262, Jan. 2011.
 - [9] C. Masouros, M. Sellathurai, and T. Ratnarajah, “Large-Scale MIMO Transmitters in Fixed Physical Spaces: The Effect of Transmit Correlation and Mutual Coupling,” *IEEE Trans. Commun.*, vol. 61, no. 7, pp. 2794–2804, July 2013.
 - [10] E. Larsson, O. Edfors, F. Tufvesson, and T. Marzetta, “Massive MIMO for Next Generation Wireless Systems,” *IEEE Commun. Mag.*, vol. 52, no. 2, pp. 186–195, Feb. 2014.
 - [11] L. Lu, G. Y. Li, A. L. Swindlehurst, A. Ashikhmin, and R. Zhang, “An Overview of Massive MIMO: Benefits and Challenges,” *IEEE J. Sel. Topics Sig. Process.*, vol. 8, no. 5, pp. 742–758, April 2014.
 - [12] C. Wang and R. D. Murch, “Adaptive Downlink Multi-user MIMO Wireless Systems for Correlated Channels with Imperfect CSI,” *IEEE Wireless Commun.*, vol. 5, no. 9, pp. 2435–2446, Sept. 2006.
 - [13] M. T. Ivrlac, W. Utschick, and J. A. Nossek, “Fading Correlations in Wireless MIMO Communication Systems,” *IEEE J. Sel. Areas Commun.*, vol. 21, no. 5, pp. 819–828, June 2003.
 - [14] D. Piazza, N. J. Kirsch, A. Forenza, R. W. Heath, and K. R. Dandekar, “Design and Evaluation of a Reconfigurable Antenna Array for MIMO Systems,” *IEEE Trans. Ant. Propag.*, vol. 56, no. 3, pp. 869–881, Mar. 2008.
 - [15] A. M. Tulino, A. Lozano, and S. Verdu, “Impact of Antenna Correlation on the Capacity of Multiantenna Channels,” *IEEE Trans. Inf. Theory*, vol. 51, no. 7, pp. 2491–2509, July 2005.
 - [16] H. Liu, Y. Song, and R. C. Qiu, “The Impact of Fading Correlation on the Error Performance of MIMO Systems over Rayleigh Fading Channels,” *IEEE Trans. Wireless Commun.*, vol. 4, no. 5, pp. 2014–2019, Sept. 2005.
 - [17] H. R. Bahrami and T. Le-Ngoc, “Precoder Design based on the Channel Correlation Matrices,” *IEEE Trans. Wireless Commun.*, vol. 5, no. 12, pp. 3579–3587, Dec. 2006.
 - [18] J. Akhtar and D. Gesbert, “Spatial Multiplexing over Correlated MIMO Channels with a Closed-form Precoder,” *IEEE Trans. Wireless Commun.*, vol. 4, no. 5, pp. 2400–2409, Sept. 2005.
 - [19] I. Gupta and A. Ksienski, “Effect of Mutual Coupling on the Performance of Adaptive Arrays,” *IEEE Trans. Ant. Propag.*, vol. 31, no. 5, pp. 785–791, Sept. 1983.
 - [20] C. A. Balanis, *Antenna Theory: Analysis and Design*, Wiley-Blackwell, 3rd edition, May 2005.
 - [21] A. A. Aouda and S. G. Haggman, “Effect of Mutual Coupling on Capacity of MIMO Wireless Channels in High SNR,” *Progress in Electro-magnetics Research*, vol. 65, pp. 27–40, 2005.
 - [22] Z. Li, Z. Du, M. Takahashi, K. Saito, and K. Ito, “Reducing Mutual Coupling of MIMO Antennas with Parasitic Elements for Mobile Terminals,” *IEEE Trans. Ant. Propag.*, vol. 60, no. 2, pp. 473–481, Feb. 2012.
 - [23] H. Aliakbarian S. Farsi, D. Schreurs, B. Nauwelaers, and G. A. E. Vandenbosch, “Mutual Coupling Reduction between Planar Antennas by Using a Simple Microstrip U-Section,” *IEEE Ant. Wireless Propag. Lett.*, vol. 11, pp. 1501–1503, 2012.
 - [24] G. Moreno, H. M. Bernety, and A. B. Yakovlev, “Reduction of Mutual Coupling between Strip Dipole Antennas at Terahertz Frequencies with an Elliptically Shaped Graphene Monolayer,” *IEEE Ant. Wireless Propag. Lett.*, vol. 15, pp. 1533 – 1536, Dec. 2015.
 - [25] J. Rubio, J. F. Izquierdo, and J. Corcoles, “Mutual Coupling Compensation Matrices for Transmitting and Receiving Arrays,” *IEEE Trans. Ant. Propag.*, vol. 63, no. 2, pp. 839–843, Feb. 2015.
 - [26] H. Steyskal and J. S. Herd, “Mutual Coupling Compensation in Small Array Antennas,” *IEEE Trans. Ant. Propag.*, vol. 38, no. 2, pp. 1971–1975, Dec. 1990.
 - [27] J. Corcoles, M. A. Gonzalez, and J. Rubio, “Mutual Coupling Compensation in Arrays using a Spherical Wave Expansion of the Radiated Field,” *IEEE Ant. Wireless Propag. Lett.*, vol. 8, pp. 108–111, Jan. 2009.
 - [28] H. T. Hui, “A Practical Approach to Compensate for the Mutual Coupling Effect in an Adaptive Dipole Array,” *IEEE Trans. Ant. Propag.*, vol. 52, no. 5, pp. 1262–1269, May 2004.
 - [29] B. Clerckx, C. Craeye, D. V.-Janvier, and C. Oestges, “Impact of Antenna Coupling on 2×2 MIMO Communications,” *IEEE Trans. Veh. Tech.*, vol. 56, no. 3, pp. 1009–1018, May 2007.
 - [30] J. Choma and W. K. Chen, *Feedback Networks: Theory and Circuit Applications*, U.S.A.: World Scientific Publishing, May 2007.
 - [31] H. A. Haus, *Electromagnetic Noise and Quantum Optical Measurements*, Springer, Nov. 2000.
 - [32] Jia-Shiang Fu, “Adaptive Impedance Matching Circuits based on Ferroelectric and Semiconductor Varactors,” *Ph.D. thesis, University of Michigan*, 2009.